ARMY RESEARCH LABORATORY

An Army Illumination Model (AAIM)

by Richard C. Shirkey

ARL-TR-4645 **November 2008**

NOTICES

Disclaimers

The findings in this report are not to be construed as an official Department of the Army position unless so designated by other authorized documents.

Citation of manufacturer's or trade names does not constitute an official endorsement or approval of the use thereof.

Destroy this report when it is no longer needed. Do not return it to the originator.

Army Research Laboratory
White Sands Missile Range, NM 88002-5501

ARL-TR-4645 **November 2008**

An Army Illumination Model (AAIM)

Richard C. Shirkey
Computational and Information Sciences Directorate, ARL

REPORT DOCUMENTATION PAGE

Form Approved
OMB No. 0704-0188

1. REPORT DATE *(DD-MM-YYYY)*	2. REPORT TYPE	3. DATES COVERED (From - To)
November 2008	Final	FY08

4. TITLE AND SUBTITLE
An Army Illumination Model (AAIM)

5a. CONTRACT NUMBER

5b. GRANT NUMBER

5c. PROGRAM ELEMENT NUMBER

6. AUTHOR(S)
Richard C. Shirkey

5d. PROJECT NUMBER

5e. TASK NUMBER

5f. WORK UNIT NUMBER

7. PERFORMING ORGANIZATION NAME(S) AND ADDRESS(ES)
U.S. Army Research Laboratory
Computational and Information Sciences Directorate
Battlefield Environment Division (ATTN: AMSRD-ARL-CI-EM)
White Sands Missile Range, NM 88002-5501

8. PERFORMING ORGANIZATION REPORT NUMBER
ARL-TR-4645

9. SPONSORING/MONITORING AGENCY NAME(S) AND ADDRESS(ES)

10. SPONSOR/MONITOR'S ACRONYM(S)

11. SPONSOR/MONITOR'S REPORT NUMBER(S)

12. DISTRIBUTION/AVAILABILITY STATEMENT
Approved for public release; distribution is unlimited.

13. SUPPLEMENTARY NOTES

14. ABSTRACT
An Army Illumination Model (AAIM), for use with Night Vision Goggles, has updated the Light Urban Model Effects (LUME) with new algorithms for cloud reflection; it also has been augmented with a population database for model input. In addition to providing illumination levels for cities, the model now includes values for lunar illumination under clear or (partially) cloudy skies at ground level. AAIM may be used in tactical decision aids and wargames for an observer at ground level, allowing for more accurate prediction of target acquisition ranges and increased realism in simulations. The original tenets of the initial model have been maintained – prediction of broadband brightness as a function of population and distance (>10 km) from city center under clear and overcast conditions. A technical overview of the model, along with future improvements, is presented.

15. SUBJECT TERMS
urban illumination, brightness distance relationship

16. SECURITY CLASSIFICATION OF:			17. LIMITATION OF ABSTRACT	18. NUMBER OF PAGES	19a. NAME OF RESPONSIBLE PERSON
a. REPORT	b. ABSTRACT	c. THIS PAGE			Richard C. Shirkey
U	U	U	UU	40	19b. TELEPHONE NUMBER (*Include area code*) (575) 678-5470

Standard Form 298 (Rev. 8/98)
Prescribed by ANSI Std. Z39.18

Contents

List of Figures

List of Tables

Acknowledgments

The author would like to recognize Dr. M.E. Cianciolo, of The Analytic Sciences Corporation, and Melanie Gouveia, of Northrop Grumman for much of the initial formulation used in the construction of this model.

Summary

An Army Illumination Model (AAIM) has been developed that estimates city brightness as a function of distance, look-angle, city population, and cloud cover for an observer at ground level. The model, which builds on the Light Urban Model Effects (LUME), has been modified to include city light reflection off of clouds and determination of lunar illumination passing through a clear or cloudy atmosphere. A database of select worldwide cities is supplied for ease of population determination. The model has been verified by comparison with external models and with measured spectral values.

INTENTIONALLY LEFT BLANK.

1. Background

Calculating the illumination from distant city lights requires knowledge of the illumination source intensity and spectra, and solving complex radiative transfer calculations to include multiple scattering by aerosols and molecular absorption in a non-homogeneous atmosphere. Currently a number of models exist for predicting urban illumination as a function of distance from urban centers at visual wavelengths or portions thereof. Since many of these models (*1–9*) were constructed primarily by members of the astronomical community to define the effects of light pollution on observatories and observation sites; they do not include the effects of clouds or cloud cover, although significant progress has been made in this area recently (*10, 11*).

The preeminent model by Garstang (*6, 7*) uses radiative transfer approximations including first and second order Rayleigh and aerosol scattering, effects of ground albedo, curvature of the earth's surface, and the areal distribution of the light source to calculate the sky light intensity. Since Garstang's model is widely mentioned in the literature and is the most comprehensive of the semi-analytical models, it is the underlying basis for An Army Illumination Model (AAIM). A brief synopsis of his model is presented in section 1.1.

1.1 Garstang's Model

Garstang's model estimates city brightness as a function of distance, look-angle, city population, and atmospheric clarity. It assumes a mostly clear atmosphere and has been shown to reproduce the observed brightness values for a wide array of cities and geometries. Garstang models the city as a uniform circle, rather than a point source, which gives better results for observers near the city and can be used for determination of the sky brightness from within the city as well. His model assumes that the city lighting produces an output represented as lumens per head of population, a fraction of which is radiated directly into the upper hemisphere. A fraction of the downward radiated fraction is reflected upward with a Lambertian distribution. The model considers the effects of an inhomogeneous atmosphere using densities of both molecules and aerosols that decrease exponentially with height. The scattered light received at the observer's position from an atmospheric elemental volume is computed by first illuminating the volume with (1) the upwelling, attenuated direct beam, and (2) first-order scattered radiance from an elemental city light source. The illuminated atmospheric elemental volume then scatters this radiation downward along the observer's line-of-sight (LOS), resulting in an attenuated radiance contribution at the observer's location. Both the city and observer may be at an arbitrary height above ground level.

1.2 AAIM

The AAIM is a highly simplified and parameterized version of Garstang's model with extensions to include cloudy skies and lunar illumination; the observer is currently located at ground level.

It does not include the brightness distribution within cities or earth curvature effects as Garstang's model does. The former, a complicated function of internal city illumination with scattering from buildings and roads, is being addressed by a 2009 Small Business Innovative Research (SBIR) proposal (*12*); for the latter, Garstang has shown that earth curvature effects are negligible for most cases where the cities are separated by a substantial distance.

To avoid redundancy only the salient points and equations found in, *A Preliminary Urban Illumination Model,* (*13*) will be presented here. Updated algorithms, particularly illumination through and reflected by clouds, are presented along with other relevant changes in the model.

Ambient illumination, which may be comprised of solar, lunar, galactic, and/or manmade lighting, strongly affects the ability of a sensor to "see" and therefore determine acquisition ranges. In nighttime warfare, the brightest sources of illumination are frequently either from the moon or urban areas. For mission planning, training purposes, and estimates of target acquisition ranges, it is necessary to have a model that will simulate natural and artificial lighting sources and then apply them to target acquisition problems such as ambient lighting conditions that vary over the course of a mission. To determine urban illumination levels due to artificial lighting, the Light Urban Model Effects (LUME) (*13*) used Walker's (*3*) brightness-distance relationship

$$B = CPD^{-\alpha}, \tag{1}$$

where B is the sky brightness, C and α are constants, P is the city population, and D is the distance from city center. This was, and still is, the basic model used.

The improved model, AAIM, consists of four major pieces for estimating the overall broadband brightness. These consist of (1) the city source, (2) lunar illumination, (3) separating the broadband city source term into its spectral components to simulate the artificial lighting spectral radiances, and (4) including effects from cloudy skies.

2. Clear Skies: LUME Review

The brightness-distance relationship, valid for a zenith-pointing look-angle, was implemented in LUME (*13*). This implementation was modified with parameterizations for C and α (equation 1) as a function of city population and added directional dependencies for city light intensity (*14*). Two corrections to the zenith brightness were made: a Gaussian drop-off in intensity in the azimuthal direction and a secant function for the zenith direction.

2.1 Estimation of Constants Used in Brightness-Distance Relationship

Garstang (*6, 7*) estimated the values of C and α and compared his results to a limited set of observations (*3*). These values were tabulated in (*14*) for a number of population categories resulting in parametric curves used for determination of C and α as a function of population:

$$\text{Log } C = 0.6323 \text{ Log } P - 2.4089, \tag{2}$$

and

$$\alpha = -0.3405 \text{ Log } P - 1.4304. \tag{3}$$

2.2 Zenith-Angle Effects

The brightness-distance relationship does not include a model for the angular effects on observed brightness. It is used to compute brightness in the zenith direction (i.e., looking straight up) only. To correct this, the effects of off-angle views and the corresponding corrections to the zenith brightness were made as follows.

To a first approximation, when viewed from far away, city lights would appear to increase in brightness as the secant of the zenith angle (*5*). To emulate this, a function was introduced to correct the zenith brightness for variations in zenith angle:

$$F(P, z) = f(z) = A(P) \sec(z), \tag{4}$$

where A is a constant of proportionality determined from empirical data and parameterized by population, P, and z is the zenith angle in degrees (the zenith angle is the complement of the elevation angle). Figure 1 defines the geometry for the zenith angle (z), azimuth angle (β) and the elevation angle ε (= $90° - z$).The constant of proportionality, A, was determined by plotting the brightness for various city populations as a function of zenith angle. For each of the cities, a best-fit secant function with its corresponding constant of proportionality, A, was determined to vary as a function of city population. The estimates of A for various populations are shown in table 1.

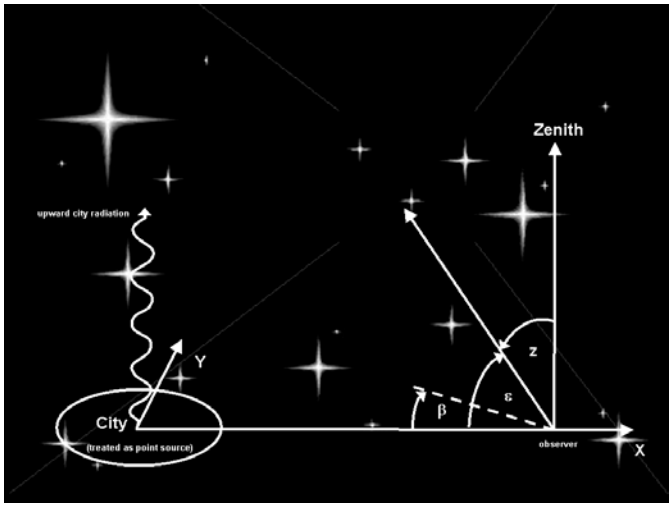

Figure 1. Geometry used in AAIM.

Table 1. Estimates of the constant of proportionality, A, and the corresponding population, P.

log P	Constant of proportionality, A
3.0	0.4
3.5	0.7
4.0	0.9
4.5	1.2
5.0	1.6
5.5	2.0
6.0	2.4
6.5	2.9

Due to the nature of the secant function approaching infinity for angles near 90°, it was only used up to 80°. For the range 80–100°, the value of the secant law valid at 80° was used. Beyond 110°, a weighted secant law is used. In summary, the zenith angle correction function, f(z), is computed as:

$$f(z) = A \sec(z), \qquad z \leq 80°, \tag{5}$$

$$f(z) = A \sec(80°), \qquad 80° < z \leq 100°, \tag{6}$$

$$f(z) = A [(1. - w) \sec(80°) + w (|(\sec(z)| - 1.)], \qquad 100° < z \leq 110°, \tag{7}$$

$$f(z) = A (|\sec(z)| - 1.), \qquad 110° < z \leq 180°, \tag{8}$$

where $w = (z - 100°) / 10$.

2.3 Azimuth-Angle Effects

For the variations in urban brightness as a function of azimuthal angle (*5*), a Gaussian weighting function was employed and defined as:

$$f(\beta)=e^{[-\beta^2/(2\gamma\sigma^2)]}, \tag{9}$$

where β is the azimuth angle ($\beta = 0°$ when looking directly at the city, $\beta = \pm 180°$ when looking directly away from the city), σ^2 is the variance of the distribution that defines the width of the Gaussian weighting function, and γ is a multiplicative factor used to modify the standard variance.

Based on qualitative observations, the variance of the Gaussian weighting function as a function of zenith angle was modified. By multiplying the variance by a variable $\gamma = \sec(90°\text{-}z)$ a new effective variance is produced resulting in a larger effective variance for small zenith angles and decreasing as the zenith angle approaches 90°. This ensures that the azimuthal dependence of the sky brightness decreases as one looks toward the zenith.

A value for the variance that results in a 50% decrease in brightness over a 30° range at a zenith angle of 90° was selected. σ^2 is then determined to be:

$$\sigma^2 = 0.19776 \text{ rad}^2. \tag{10}$$

In summary, the azimuth angle correction function is computed in two steps. First, determination of the value for γ used to modify the variance:

$$\gamma = 1.0 / \cos(90° - z) \quad \text{for} \quad 0° < z \leq 90°, \tag{11}$$

and

$$\gamma = 1.0 \qquad \text{for} \quad 90° < z \leq 180°, \tag{12}$$

then calculate the function itself:

$$f(\beta)=e^{[-\beta^2/(2\gamma\sigma^2)]}. \tag{13}$$

After identifying the correction factors for the change in brightness due to zenith and azimuth angle effects, the broadband brightness from the city is calculated by combining equations 1, 4, and 13:

$$B = CPD^{-\alpha} f(z) f(\beta) \tag{14}$$

3. Population and Location Database

As an upgrade to LUME, and since population is an integral input for the model, a limited database (cities info.txt) is provided with the program to supply not only the population of various worldwide cities, but also their latitude and longitude in decimal degrees (the degrees, minutes, seconds (DMS) format is not supported). Given that the population is the main driver of city illumination, where possible the metropolitan area population, rather than the city population itself, was used. The available cities, as well as their latitude and longitude, may be found in appendix A and in the supplied cities info.txt data base. These latter two quantities are needed for determination of lunar phase and illumination at the top of the atmosphere. If the user desired city is not in the database, the user is asked to enter the population and latitude and longitude of that city, which may be optionally entered into the database by the user. The latitude and longitude and population for worldwide cities may be found at http://www.world-gazetteer.com/.

4. Lunar Illumination under Clear and Cloudy Skies

Prediction of lunar illumination under realistic atmospheric conditions that include clear skies, partly cloudy and overcast conditions, precipitation, and fog is handled by a modified version of the ILUMA model (*15*): a simple two stream radiative transfer model with three layers of atmosphere. Each layer is represented in terms of the cloud amount and cloud thickness or type. An albedo option allows one to account for realistic albedo conditions of the ground surface. Illumination is computed only for the moon; background sky effects (zodiacal light, starlight, etc.) are not included at this juncture.

The calculation of transmission of visible light through the atmosphere is based upon a three-layer radiative transfer model developed by Shapiro (*16*). The methodology combines a simple two-stream approximation in conjunction with tabulated mean climatological reflection and transmission coefficients. In the doubling method used by Shapiro, the reflection and transmission function of the layer consisting of n sublayers is computed by means of the known reflection and transmission functions in the separate layers. The three layer case is the simplest geometry that makes use of the standard cloud code information which categorizes clouds into high, middle, and low cloud types.

The calculation of the lunar illuminance, taken as 0.267 lm m^{-2} for the moon in the zenith on a clear night, is based upon the procedure used by van Bochove (*17*). Illuminance as a function of the phase of the moon is based on the results of Russell (*18*).

ILUMA calculates the effect of cloud cover on illumination level by using traditional surface observations that report the type of cloud and percent cloud cover in the standard low, middle and upper levels. The input for the three layer model consists of the cloud base height and type for the three layers, the cloud fraction for each layer, and the surface albedo (reflectivity). Within these three levels Shapiro found that there was little difference between some of the cloud types and classified them into four cloud groups: cirrus (Ci)/cirrostratus (Cs), altostratus (As)/altocumulus (Ac), cumulus (Cu)/cumulonimbus (Cb), and stratus (St)/stratocumulus (Sc). The overall layer scheme is as follows:

- High - clear, thin and thick Ci/Cs
- Medium - clear, As/Ac
- Low - clear, clear (f/k), Cu/Cb or St/Sc

where (f/k) indicates fog or smoke reported. For clear skies, the fractional cloud amount for each layer is set to zero.

5. Illumination Due to City Lights Under Cloudy Skies

The brightness reflected from the cloud layer due to city lighting was calculated under a non-scattering atmosphere with an extinction coefficient of 0.15 km^{-1}, which equates to a visibility of ~ 25 km. The total light output from the city is assumed to be LP lumens, where L is the lumens per head of the population, P. A value of L = 1000 was used (*6*). No provision is made for shielding by luminaries. Simple attenuation is carried out over the two paths considered – upward from the city and downward along the observer's LOS. The brightness was further modified by using the previous correction factors for falloff in both the zenith and azimuthal directions. The resulting equation is

$$B=\frac{LP}{\pi h^2 r^2}\cos(z)\cos(\theta)^2 f(z) f(\beta)\rho(z)\, e^{-\tau_1} e^{-\tau_2}, \qquad (15)$$

where h and r are the distances along the LOS from the city to the cloud base and from the observer's LOS to the cloud base, respectively; z is the zenith angle; θ is the angle between the city's zenith and its LOS; ρ is the cloud and angle dependent reflectivity (assumed to be Lambertian); and the optical depths along the paths considered are τ_1 = k h and τ_2 = k r, where k is the extinction coefficient in km^{-1}. Figure 2 presents the geometry; b is the cloud base height; and d is the distance from the observer to city center.

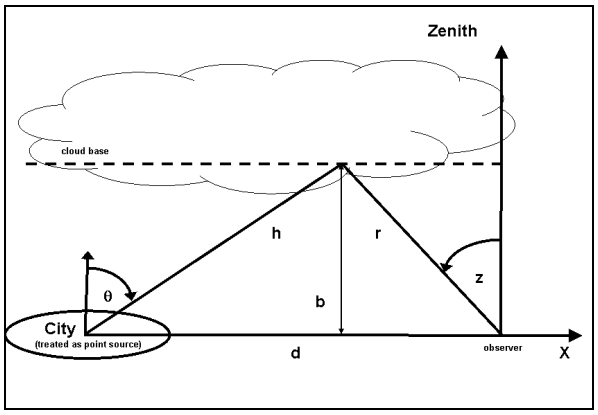

Figure 2. Geometry used for cloud cases.

Note: the cloud base is indicated by the dashed line

6. Spectral Composition of the Broadband Brightness

The spectral composition of urban light is determined by identifying the types of lights used in typical cities and estimating the percentage that each light source contributes to the overall city light source. While the lunar illumination is included in the total broadband brightness, it is not currently included in the spectral values. The spectral radiance values over the sensor's waveband are calculated based on the city brightness amount due to each individual light source. The method for accomplishing this is discussed in section 6.1.

6.1 City Light Types and their Spectral Composition

The types of lights that comprise urban settings and their spectral content must be known for the model to function, i.e., an illumination database of some nature is required. In any given city many light types are employed on city streets, highways, office buildings, shopping centers, stadiums, houses, parking lots, etc. The resulting mix of light is highly heterogeneous due to the variety of light source spectra, the effects of atmospheric scattering and absorption, and reflection from the ground. The mix contains both a broad continuum of radiation along with many superimposed emission lines at specific wavelengths. From 300–500 nm, a pseudo continuum is formed by the many emission lines of the mercury vapor and multivapor lights (*19*). Beyond 500 nm, metal halide and high pressure sodium lamps are the primary contributors to the city light continuum.

In AAIM, a given mix of light sources was assumed and the proportion of light that is provided by each type was estimated from lighting data taken for El Paso, TX and Las Cruces, NM (*20*), and broken down into individual light types by percent. The results are presented in table 2.

Table 2. Breakdown of Street and flood lights in El Paso, TX and Las Cruces, NM in 2007.

Light Type	Percent of total light
Clear mercury Street	20.2%
High pressure sodium	77.9% Street 63.3% Area Floods 14.6%
Medal Halide Floods	1.9 %
Total	100 %

Using the lighting percentages in table 2, the amount of the brightness due to each light type is determined by multiplying the broadband brightness by each percentage. For example, $B_{\text{high pressure sodium}} = B \times 0.779$, etc.

Each of the three light types listed in table 2 has a characteristic spectral distribution shown in figure 3. Spectral distributions for these light types (*21, 22*) were used along with general knowledge of each light's emission lines and continuum to build light spectra for the range 300–1100 nm at 10 nm resolution. These distributions were digitized for each of the three light types and coded into the model.

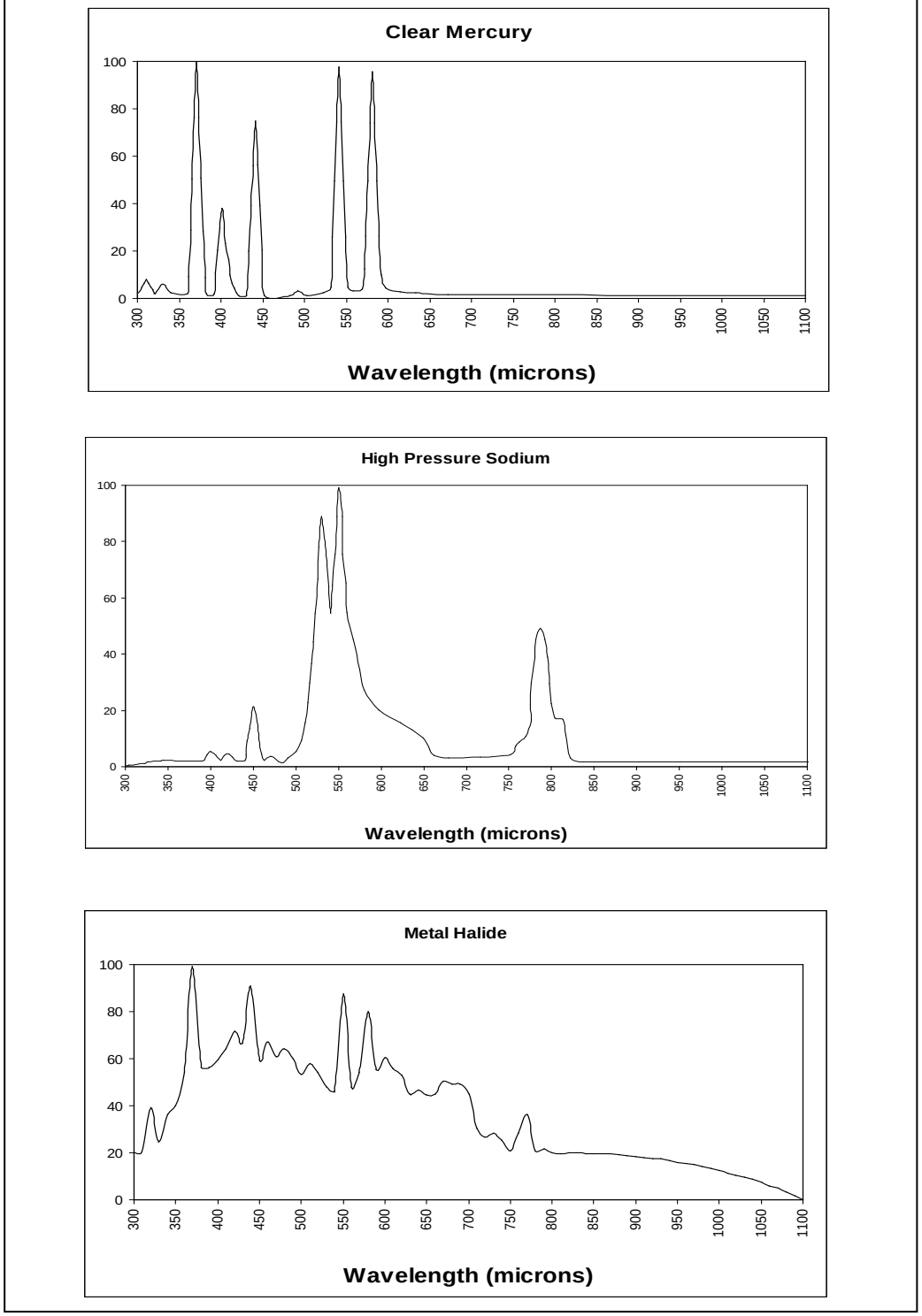

Figure 3. Spectra of light sources in table 2.

6.2 Radiant Energy Determination

The total radiant energy (in relative units) for each light type was computed by summing the area under the spectrum over the entire wavelength range for a given light type (300–1100 nm). The total radiant energy, E_i, for the specific light type (specified by the index *i*) is thus given by

$$E_i = \sum_{\lambda=300}^{1100} e_{i\lambda} \Delta\lambda \,, \tag{16}$$

where $e_{i\lambda}$ is the radiant energy at a specific wavelength taken from the digitized spectra and $\Delta\lambda$ is the bin width which is taken here as 10 nm. This quantity is precomputed for use in the code. The radiant energy (in relative units) corresponding to a specific wavelength band (specified by the index λ) is computed similarly, where the sum is over the user supplied wavelengths of interest, defined by λ_{min} and λ_{max}:

$$E_{i\lambda} = \sum_{\lambda_{min}}^{\lambda_{max}} e_{i\lambda} \Delta\lambda \,. \tag{17}$$

Finally, the broadband brightness can be separated into its spectral components by summing the contributions from each of the light types to each spectral band. The total city brightness in a wavelength band defined by λ_{min} and λ_{max} is calculated as follows:

$$B_\lambda = \sum_{i=1}^{3} \frac{E_{i\lambda}}{E_i} B_i \tag{18}$$

where B_i is the proportion of the city broadband brightness associated with a specific light type.

6.3 Convert Brightness to Radiance Units

The final step in calculating the radiance contribution due to urban illumination is to convert from photometric units (nL) to radiometric units ($W/m^2/sr/\mu m$). In this case, we first converted to $nL/\mu m$ by normalizing the spectral radiance value computed above by the width of the wavelength interval in microns. Equation 19 was used for the final conversion:

$$B\ (W/m^2/sr/\mu m) = B\ (nL/\mu m) \times 1.464 \times 10^{-8}. \tag{19}$$

7. Validation

7.1 Clear Atmosphere

The results for lunar illumination at the surface were compared with results from ILUMA and found to be in agreement. The results from AAIM were compared to an equivalent formulation by Albers (*8*). Since his model is only valid for the brightness at the zenith, comparisons were

made for a zenith and azimuthal angles of zero, with no correction factors considered. The results of the two models agreed to a factor less than 2.

Validation was also done via comparison with results from Garstang (*6*). His figures 2 and 3 were digitized and compared with AAIM values computed for the same location and geometries. Figure 4 shows brightness as a function of zenith angle for the city of Denver; the distance was fixed at 40 km. Garstang's values were converted from magnitude/arcsec^2 to nL using his equation 19, and presented here as equation 20.

$$B = 34.08 \exp (20.7233 – 0.92104 V), \quad (20)$$

where V is the visual magnitude of the sky in magnitude/arcsec^2 and B is the is the sky brightness in nL. Garstang's figure 3 was also compared with AAIM with results presented in figure 5.

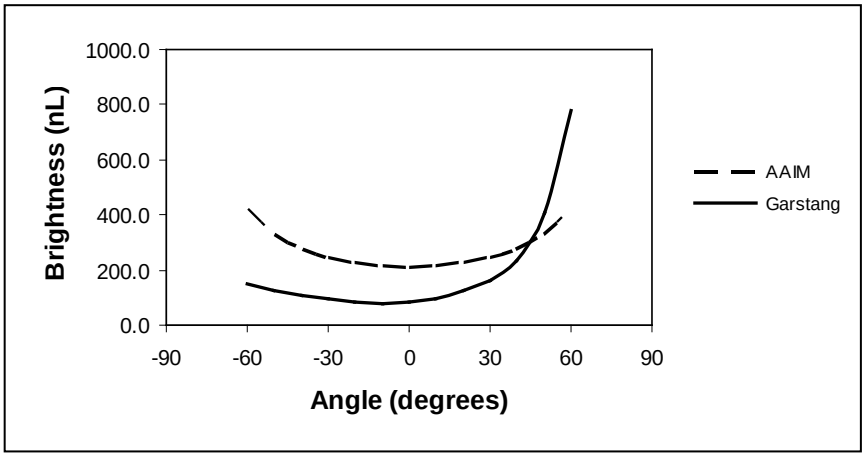

Figure 4. Sky brightness due to Denver as a function of zenith angle at a distance of 40 km.

Note: No lunar illumination values are included.

Considering that AAIM does not account for scattering processes, the results are reasonable and allows confidence that the model produces reasonable results.

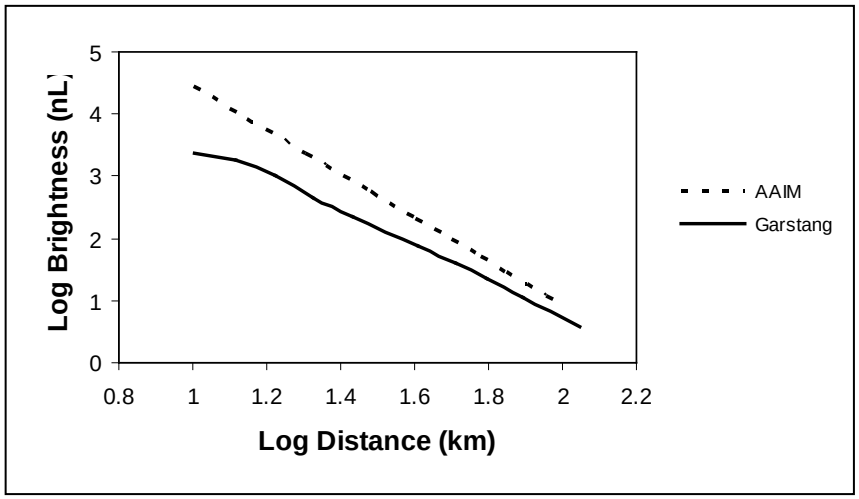

Figure 5. Sky brightness due to Denver as a function of distance for a zenith angle of zero.

Note: No lunar illumination values are included.

Spectral results were compared to those of Aube (*25*) who measured a zenith brightness of 0.3×10^{-5} w m^{-2} μm^{-1} sr^{-1} at Mt. Palomar Observatory, CA on a moonless night in May of 2005. Running AAIM for the same parameters at a distance of 120 km from Los Angeles, CA we find a value of 0.34×10^{-5} w m^{-2} μm^{-1} sr^{-1}. This almost exact agreement must be tempered by the fact that the greater Los Angeles area extends at least halfway to Mt. Palomar.

7.2 Cloudy Atmosphere

The spectral output under cloudy skies was compared with that of Desrochers and Hiett (*26*) who measured sky glow on a moonless night under cloudy conditions at Hanscom Air Force Base (HAFB), approximately 25 km outside of Boston, MA. The observed base heights ranged from 0.3 km to 1.0 km and their figure 2 shows a broad peak from about 550 to 650 nm and another highly peaked region at ~825 nm. These two peaks correspond well with the spectral lines of high pressure sodium lamps (see figure 3). If we ignore those two peaks, we get an eyeball average of 0.25×10^{-3} w m^{-2} μm^{-1} sr^{-1} (Note: there is some confusion as to their ordinate scale, which is assumed here to be scaled up by a factor of 10^4). By running AAIM and using input values from (*26*), i.e., a distance of 25 km from Boston on 16 February 1998, at 0400 coordinated universal time (UTC) under a overcast sky comprised of Sc/St clouds with a base of 1.1 km, we find a value of 0.30×10^{-5} w m^{-2} μm^{-1} sr^{-1}. This discrepancy of two orders of magnitude could easily be because their location on HAFB was only partly shielded from local light sources. If we reduce the distance to 12.5 km, thereby simulating an increase in lighting brightness, we find a value of 0.41×10^{-3} w m^{-2} μm^{-1} sr^{-1} in good agreement with their values. Finally, a quote from Garstang (*27*) would seem appropriate here: “Since the two sites are so close to each other, the disparity between the zenith brightnesses indicate that very local lighting is relatively more predominant than is accounted for in many sky brightness models.”

8. Program Usage

Depending upon the options chosen, the program provides:

- Sky brightness due to city lights in a clear atmosphere
- Sky brightness due to city lights under cloudy skies
- Lunar brightness in a clear atmosphere
- Lunar brightness under cloudy skies
- Spectral radiance of city lights in a clear atmosphere
- Spectral radiance of city lights under cloudy skies.

The program requires user input be either interactive or file-directed. To become familiar with usage of the program, default values are provided (table 3). The required inputs are the beginning/ending sensor wavelength (μm), country and city of interest, zenith and azimuth angles (degrees), horizontal distance from the observer to the city (km), date and time (UTC), and the ground albedo (see table 4 for some representative values *(15)*). In addition, when clouds are of interest, additional required inputs are cloud type (table 5), and cloud fraction amounts for the three layers. The average cloud base heights needed to determine the vertical distance of the city light reflection from the cloud base are internally selected from the four available cloud categories. If so desired, the user may change the cloud base height for the cloud type selected. Cloud reflection coefficients are provided through ILLUMA and are based on the work of Shapiro (*16*). The latitude and longitude for the location is obtained from the city database discussed elsewhere in this document.

Table 3. Program inputs and their default values (from *(15)*).

Input	Default Value
Beginning/ending wavelength	0.6 - 0.9 μm
City/Country	Boston, US
Date	2 February 2008
UTC	0200
Surface Albedo	0.25
State of cloudiness: High - no clouds Middle - no clouds Low - overcast with Cu/Cb	
Zenith angle	10.0°
Azimuth angle	0.0° (towards city center)
Distance from city center	25 km

Table 4. Albedos of various surfaces.

Soils	**Dry**	**Wet**	**Unspecified**
Dark	0.13	0.08	
Light	0.18	0.10	
Dark-ploughed	0.08	0.06	
Light-ploughed	0.16	0.08	
Clay	0.23	0.16	
Sandy	0.25	0.18	
Sand	0.40	0.20	
White sand	0.55		
Surfaces			
Asphalt			0.10
Lava			0.10
Tundra			0.20
Steppe			0.20
Concrete			0.30
Stone			0.30
Rock	0.35		0.20
Dirt road	0.25		0.18
Clay road	0.30		0.20
Fields	**Growing**	**Dormant**	
Tall grass	0.18	0.l3	
Mowed grass	0.26	0.19	
Deciduous trees	0.18	0.12	
Coniferous trees	0.14	0.12	
Rice	0.12		
Beet wheat	0.18		
Potato	0.19		
Rye	0.20		
Cotton	0.21		
Lettuce	0.22		
Snow			
Fresh	0.85		
Dense	0.75		
Moist	0.65		
Old	0.55		
Melting	0.35		
Ice			
White	0.75		
Grey	0.60		
Snow and ice	0.65		
Dark glass	0.10		

Table 5. Cloud base heights for cloud types in AAIM.

Level	Cloud Type	Cloud Base (km)
High	Ci/Cs	9.3 *
Middle	As/Ac	4.0†
Low	Cu/Cb	1.2 †
Low	Sc/St	1.1†

* ref 23
† ref 24

The user will be asked to provide the population and latitude and longitude, if a city/country is not in the supplied database (cities info.txt). This user supplied city information can then be added to the database for future reference, if desired.

Depending on the options chosen, the program will provide values for the city and lunar broadband brightness, or cloud reflected city and transmitted lunar brightness in nL. Spectral values are provided in units of $W/m^2/\mu m/sr$. Lunar illumination is not included in the spectral output, but will be incorporated in the next version. For comparison purposes, when either the default values or clouds are selected, the program provides the cloud reflected brightness for an observer looking directly at the city center zenith.

Finally, two sample input files are provided for file-directed input usage, one for full moon (full_moon.dat) and one for new moon values (new_moon.dat).

9. Conclusion

This model builds on previous research that predicts the broadband brightness as a function of population and distance from the city center. To that distance-based model, azimuth and zenith dependencies are added to predict changes to the brightness for off-angle viewing directions. The ability to calculate illumination from either city or lunar sources has been included and reflection and transmission due to clouds is considered. Finally, the types of light sources employed in urban lighting have been updated to current usage. These data define the spectral composition of the broadband illumination.

This model is simple and fast. Several caveats concerning the model are compiled here. The current model caveats are as follows:

- The broadband brightness model developed for visual waveband is assumed to hold true for near-infrared too.
- Model parameters are selected for a single atmospheric state.
- Cities are treated as point sources.

10. Future Work

Future efforts will include the following:

- Separating the lunar illumination into spectral components
- Allowing for a variable turbid atmosphere
- Inclusion of single scattering effects
- Shielding by luminaries
- Addition of background light (zodiacal, etc.)
- Addition of foreign city light types
- Comparison with the World Atlas of the Artificial Night Sky Brightness (*28*)
- Allowing city reflection from partially cloudy skies
- Extend light type spectra to near-IR wavelengths
- Allow the observer to be located at an arbitrary height above ground level

11. References

1. Walker, M. F. The California Site Survey. *Publ. Astron. Soc. Pacific* **1970**, *82*, 672–698.
2. Walker, M. F. Light pollution in California and Arizona. *Publ. Astron. Soc. Pacific* **1973**, *85*, 508–519.
3. Walker, M. F. The Effects of Urban Lighting on the Brightness of the Night Sky. *Publ. Astron. Soc. Pacific* **1977**, *89*, 405–409.
4. Treanor, P. J. A Simple Propagation Law for Artificial Night-Sky Illumination. *The Observatory* **1973**, *93*, 117–120.
5. Berry, R. L. Light Pollution in Southern Ontario. *Journal of the Royal Astronomical Society of Canada* **1976**, *70* (3), 97–115.
6. Garstang, R. H. Model for Artificial Night-Sky Illumination. *Publ. Astron. Soc. Pacific* **1986**, *98*, 364–375.
7. Garstang, R. H. Night-Sky Brightness at Observatories and Sites. *Publ. Astron. Soc. Pacific* **1989**, *101*, 306–329.
8. Albers, S.; Duriscoe, D. Modeling Light Pollution from Population Data and Implications for National Park Service Lands. *The George Wright Forum* **2001**, *18* (3).
9. Aubé, M.; Franchomme-Fossé, L.; Robert-Staehler, P.; Houle, V. Light Pollution Modeling and Detection in a Heterogeneous Environment: Toward a Night Time Aerosol Optical Depth Retrieval Method. *Proc. of SPIE* **2005**, 5890.
10. Kocifaj, M. Light-Pollution Model for Cloudy and Cloudless Night Skies with Ground-Based Light Sources. *Applied Optics* **2007**, *46*, 15.
11. Kocifaj, M. Light Pollution Simulations for Planar Ground-Based Light Sources (preprint). *Applied Optics* **2008**.
12. http://www.dodtechmatch.com/DOD/Opportunities/SBIRView.aspx?id=A08-057&page=print (accessed October 2008).
13. Shirkey, R. C. *A Preliminary Illumination Model*; ARL-TR-4320; U.S. Army Research Laboratory: WSMR, NM, 2007 (DTIC No. ADA474479).
14. Gouveia, M. J.; Cianciolo, M. E.; Higgins, G. J. *Night Vision Goggles Operations Weather Software (NOWS)*; AFRL-VS-TR-2001-1580; U.S. Air Force Research Laboratory: Hanscom AFB, MA, 2000.

15. Duncan, L. D.; Sauter, D. P.; Miller, A. *Natural Illumination Under Realistic Weather Conditions, ILUMA*; ASL-TR-0221-21; EOSAEL 87, Vol 21; U.S. Atmospheric Sciences Laboratory: WSMR, NM, October 1987.

16. Shapiro, R. *Solar Radiative Flux Calculations from Standard Surface Meteorological Observations*; AFGL-TR-82-0039; U.S. Air Force Geophysical Laboratory: Hanscom AFB, MA, 1982 (DTIC No. ADA118775).

17. van Bochove, A. C. *The Computer program ILLUM: Calculation of the Position of Sun and Moon and the Natural Illumination*; PHL 1982-13; Physics Laboratory TNO, The Hague, The Netherlands; 1982.

18. Russell, H. N. The Stellar Magnitude of the Sun, Moon and Planets. *Astrophysical Journal* **1916**, *43*, 103–129.

19. Lane M. C.; Garrison R. G. The Night-Sky Spectrum of the City of Toronto. *Journal of the Royal Astronomical Society of Canada* **1978**, *72* (4), 198–205.

20. Private communication, El Paso Electric Co., El Paso, TX, 2007.

21. Finch, D. M. Atmospheric Light Pollution. *Journal of the Illuminating Engineering Society* **1978**, *7* (2), 105–117.

22. http://www.highend.com/support/training/metalhalide.asp (accessed October 2008).

23. Jursa, A. S. Ed.; *Handbook of Geophysics and the Space Environment*; Air Force Geophysics Laboratory, 1985; pp 16–44 (DTIC No. ADA 167000).

24. Low, R.D.H. *Cloud Transmission Module CLTRAN*; ASL-TR-0221-9; U.S. Army Research Laboratory: WSMR, NM, 1987 (DTIC No. ADB332821).

25. Aube, 2009, http://www.graphycs.qc.ca/aubema/recherches/data/Data/north-america/usa/california/mount-palomar/2005/palomar-zenith-may-2005.png (accessed October 2008).

26. Desrochers, P. R.; Hiett, T. Cloud impacts on urban glow. *29th International Conference on Radar Meteorology*; Montreal, Canada; United States; 12–16 July 1999; pp 436-439.

27. Narisada, K.; Schreuder, D. *Light Pollution Handbook*, Astrophysics and Space Science Library, Vol 322; Springer, The Netherlands; 2004, pp 861 (ISBN 1-4020-2665-X (HB); 1-4020-2668-8 (e-book)).

28. Cinzano, P.; Falchi, F.; Elvidge, C. D. The First World Atlas of the Artificial Night Sky Brightness. *Mon. Not. R. Astron. Soc.* **2001**, *328*, 689–707.

INTENTIONALLY LEFT BLANK.

Appendix A. Population of Select Worldwide Cities (Metropolitan areas used when available.)

Population	Country	City	Latitude	Longitude
349000	Afghanistan	Herat	34.333	62.200
2536300	Afghanistan	Kabul	34.517	69.200
324800	Afghanistan	Quandahar	30.996	65.476
300600	Afghanistan	Mazar-e Sharif	67.110	67.110
56200	Afghanistan	Baghlan	36.120	68.703
300000	Albania	Tirane	41.332	19.817
4447000	Algeria	Algier	36.775	3.060
22390	Andorra	Andorra la Vella	42.500	1.500
2000000	Angola	Luanda	13.232	13.232
21514	Antigua and Barbuda	St. John's	17.118	–61.846
12431000	Argentina	Buenos Aires	–34.667	–58.500
1315500	Argentina	Córdoba	18.917	–96.917
1226000	Armenia	Yerevan	40.167	44.517
29998	Aruba	Oranjestad	12.517	–70.033
1040719	Australia	Adelaide	–34.917	138.583
21622	Australia	Alice Springs	–23.700	133.883
1676389	Australia	Brisbane	–27.467	153.033
307700	Australia	Canberra	–35.283	149.133
66291	Australia	Darwin	–12.467	130.833
3188000	Australia	Melbourne	144.963	144.963
1256035	Australia	Perth	–31.933	115.833
3665000	Australia	Sydney	–33.867	151.207
128808	Australia	Townsville	–19.217	146.800
1600000	Austria	Vienna	48.200	16.367
1713300	Azerbaijan	Baku	40.367	49.883
171542	Bahamas	Nassau	25.066	–77.339
155000	Bahrain	Al-Manamah	26.217	50.567
140401	Bahrain	Manama	26.215	50.588
10979000	Bangladesh	Dhaka	23.717	90.417
6700	Barbados	Bridgetown	13.100	–59.617
1666000	Belarus	Minsk	53.850	27.500
949070	Belgium	Brussels	50.833	4.333
5845	Belize	Belmopan	17.217	–88.800
30340	Bhutan	Thimphu	27.533	89.717
713400	Bolivia	La Paz	–16.500	–68.167
310000	Bosnia	Sarajevo	43.850	18.383
138000	Botswana	Gaborone	–24.750	25.917
1800000	Brazil	Brasília	–15.783	–47.917
3699000	Brazil	Porto Alegre	–30.028	–51.229
3307000	Brazil	Recife	–8.100	–34.883

Population	Country	City	Latitude	Longitude
10556000	Brazil	Rio de Janeiro	–22.900	–43.233
3180000	Brazil	Salvador	–12.963	–38.512
17711000	Brazil	Sao Paulo	–23.533	–46.617
52300	Brunei	Bandar Seri Begawa	4.883	114.933
1113674	Bulgaria	Sofia	42.667	23.300
500000	Burkina	Ouagadougou	12.367	–1.517
300000	Burundi	Bujumbura	–3.367	29.317
900000	Cambodia	Phnom Penh	11.550	104.917
1299446	Cameroun	Yaound	3.850	11.583
3401000	Canada	Montreal	45.545	–73.639
1130761	Canada	Ottawa	45.417	–75.717
24570	Canada	Riviere-du-Loup	–69.269	–69.269
715515	Canada	Quebec	46.833	–71.250
233923	Canada	Saskatoon	52.167	–101.533
4657000	Canada	Toronto	43.650	–79.383
2116581	Canada	Vancouver	49.267	–123.117
5113149	Canada	Toronto	43.670	–79.387
694668	Canada	Winnipeg	49.883	–97.150
61797	Cape Verde	Praia	14.917	–23.517
529555	Chad	N'Djamena	12.167	14.983
5261000	Chile	Santiago	–33.450	–70.667
12033000	China	Beijing	39.917	116.433
5566000	China	Changchun	43.887	125.325
5293000	China	Chengdu	30.711	104.088
3896000	China	Chongging	29.555	106.548
3153000	China	Dalian	38.914	121.616
5162000	China	Guangzhou	23.127	113.342
3763000	China	Handan	36.610	114.481
6389000	China	Hangzhou	30.274	120.173
5475000	China	Harbin	45.750	126.683
6097000	China	Hong Kong	22.320	114.239
4789000	China	Jinan	36.665	116.995
3375000	China	Nanjing	32.056	118.798
4376000	China	Qingdao	36.108	120.416
14173000	China	Shanghai	31.100	121.367
5681000	China	Shenyang	41.828	123.416
10239000	China	Tianjin	39.104	117.252
4750000	China	Wuhan	30.583	108.900
3352000	China	Xi'an	34.265	108.944
6834000	Colombia	Bogota	4.600	–74.083
3831000	Colombia	Medellin	6.251	–75.576
937580	Congo	Brazzaville	4.233	15.233
5068000	Congo	Kinshasa	–4.300	15.300
315909	Costa Rica	San Jose	9.933	–84.083
3359000	Cote d'Ivoire	Abidjan	5.317	–0.083
930753	Croatia	Zagreb	45.800	15.967
2241000	Cuba	Havana	23.133	–82.367

Population	Country	City	Latitude	Longitude
186400	Cyprus	Nicosia	35.167	33.367
1215771	Czech Republic	Prague	50.100	14.433
1339395	Denmark	Copenhagen	55.750	12.417
395000	Djibouti	Djibouti	11.550	43.167
15853	Dominica	Roseau	15.300	–61.383
3601000	Dominican Republic	Santo Domingo	18.467	–69.900
1500000	Ecuador	Quito	–0.233	–78.500
3995000	Egypt	Alexandria	31.214	29.944
150000	Egypt	Aswan	24.083	32.933
10772000	Egypt	Cairo	30.050	31.250
972810	El Salvador	San Salvador	13.667	–89.167
400000	Eritrea	Asmara	15.333	38.967
471608	Estonia	Tallinn	59.433	24.717
2200186	Ethiopia	Addis Ababa	9.050	38.700
2115	Falkland Islands	Stanley	–51.750	–57.933
200000	Fiji	Suva	–18.133	178.417
515765	Finland	Helsinki	60.133	25.000
630000	France	Bordeaux	44.833	–0.567
347900	France	Nice	43.700	7.250
9638000	France	Paris	48.867	2.333
419596	Gabon	Libreville	0.500	9.417
44188	Gambia	Banjul	13.467	–16.650
1279000	Georgia	T'bilisi	41.717	44.817
3471418	Germany	Berlin	52.533	13.417
3251000	Germany	Dusseldorf	51.225	6.776
6559000	Germany	Essen	51.458	7.015
3700000	Germany	Frankfurt	50.112	8.681
82220000	Germany	Hamburg	53.550	9.983
3067000	Germany	Koln	50.941	6.960
3200000	Greece	Athens	37.967	23.717
3103000	Greece	Athina	37.979	23.717
4439	Grenada	St. George's	12.067	61.733
160000	Guam	Hagatna	13.467	144.750
1150452	Guatemala	Guatemala City	14.633	–90.517
1508000	Guinea	Conakry	9.483	–13.717
200000	Guinea-Bissau	Bissau	11.867	–15.650
248500	Guyana	Georgetown	6.800	–58.167
1500000	Haiti	Port Au Prince	18.533	–72.333
310000	Herzegovina	Sarajevo	43.850	18.383
1500000	Honduras	Tegucigalpa	14.083	–87.233
4160000	Brazil	Belo Horizonte	–19.816	–43.954
2008546	Hungary	Budapest	47.500	19.083
103036	Iceland	Reykjavik	–64.150	21.850
4154000	India	Almadabad	72.566	72.566
5544000	India	Bangalore	12.967	77.583
12900000	India	Calcutta	22.500	88.333
6639000	India	Chennai	13.060	80.250

Population	Country	City	Latitude	Longitude
11680000	India	Delhi	28.667	77.233
6833000	India	Hyderabad	17.385	78.487
18042000	India	Mumbai	18.933	74.583
294149	India	New Delhi	28.635	77.225
3485000	India	Pune	18.520	73.857
3420000	Indonesia	Bangdung	–6.912	107.607
11500000	Indonesia	Jakarta	–6.133	106.750
2410800	Iran	Mashad	36.267	59.567
1204882	Iran	Shiraz	29.633	52.567
1378935	Iran	Tabriz	38.083	46.300
7705036	Iran	Tehran	35.667	51.433
313552	Iraq	Ad-Diwaniyah	31.978	44.900
333142	Iraq	Al-'Amarah	31.830	47.148
1100790	Iraq	Al-Basrah	30.293	47.292
428933	Iraq	Al-Hillah	32.497	44.446
292274	Iraq	Al-Kut	32.529	45.828
1174022	Iraq	Al-Mawsil	36.340	43.144
502842	Iraq	An-Najaf	31.352	44.096
424311	Iraq	An-Nasiriyah	31.039	46.236
910381	Iraq	Arbil	36.557	44.385
307229	Iraq	Ar-Ramadi	33.432	43.312
119665	Iraq	As-Samawah	43.281	43.281
683261	Iraq	As-Sulaymaniyah	45.450	45.450
6956562	Iraq	Baghdad	33.333	44.433
183486	Iraq	Ba'qubah	33.747	44.662
1100790	Iraq	Basra	30.520	47.824
910381	Iraq	Irbil	36.180	44.016
454090	Iraq	Karbala'	32.406	43.867
618149	Iraq	Kirkuk	35.468	44.395
1174022	Iraq	Mosul	36.335	43.137
2550500	Israel	Jerusalem	31.783	35.217
380000	Israel	Tel Aviv	32.066	34.778
364779	Italy	Florence	43.767	11.250
4251000	Italy	Milano	45.464	43.137
993400	Italy	Naples	40.850	14.283
3012000	Italy	Napoli	40.840	14.253
2693383	Italy	Rome	41.800	12.600
104000	Jamaica	Kingston	17.967	–76.800
1157846	Japan	Hiroshima	34.383	132.450
3377000	Japan	Nagoya	35.156	136.916
10609000	Japan	Osaka	34.678	135.507
28025000	Japan	Tokyo	35.667	139.750
963490	Jordan	Amman	31.950	35.933
280200	Kazakhstan	Astana	51.167	71.500
193300	Kazakhstan	Petropavl	54.883	69.217
2000000	Kenya	Nairobi	–1.283	36.817
151060	Kuwait	Kuwait City	29.333	48.000

Population	Country	City	Latitude	Longitude
631000	Kyrgyzstan	Bishkek	42.883	74.767
442000	Laos	Vientiane	17.967	102.600
874000	Latvia	Riga	56.667	106.167
1100000	Lebanon	Beirut	33.867	35.500
170000	Lesotho	Maseru	–29.317	27.483
1000000	Liberia	Monrovia	6.300	–10.783
950000	Libya	Benghazi	32.117	20.067
1682000	Libya	Tripoli	32.900	13.183
5067	Liechtenstein	Vaduz	47.133	9.533
590100	Lithuania	Vilnius	54.683	25.317
75622	Luxembourg	Luxembourg	49.617	6.133
444229	Macedonia	Skopje	42.000	21.467
1000000	Madagascar	Antananarivo	–18.867	47.500
260000	Malawi	Lilongwe	–13.967	33.817
1145000	Malaysia	Kuala Lumpur	3.133	101.700
62973	Maldives	Male	4.174	135.507
746000	Mali	Bamako	12.650	–8.000
9183	Malta	Valletta	35.900	14.533
20000	Marshall Islands	Majuro	7.083	171.133
480000	Mauritania	Nouakchott	18.150	–15.967
134516	Mauritius	Port Louis	–20.167	57.500
3908000	Mexico	Guadalajara	20.667	–103.333
18131000	Mexico	Mexico City	19.400	–99.150
3416000	Mexico	Monterrey	25.685	–100.305
676700	Moldova	Chisinau	47.000	28.833
30400	Monaco	Monaco	43.750	7.383
619000	Mongolia	Ulan Bator	47.900	106.867
3535000	Morocco	Casablanca	33.589	–7.609
1220000	Morocco	Rabat	34.033	–6.850
3017000	Mozambique	Maputo	–25.967	32.583
4458000	Myanmar (Burma)	Yangon	16.783	96.167
161000	Namibia	Windhoek	–22.567	17.100
535000	Nepal	Kathmandu	27.700	85.317
724096	Netherlands	Amsterdam	52.350	4.900
1208091	New Zealand	Auckland	–36.917	174.783
397974	New Zealand	Wellington	–41.283	174.783
974000	Nicaragua	Managua	12.100	–86.300
398265	Niger	Niamey	13.533	2.083
339000	Nigeria	Abuja	9.167	7.183
13488000	Nigeria	Lagos	6.450	3.400
2741260	North Korea	Pyongyang	39.000	125.783
483401	Norway	Oslo	59.917	10.750
350000	Oman	Muscat	23.617	58.633
201000	Pakistan	Islamabad	33.667	73.133
11774000	Pakistan	Karachi	24.850	67.033
6030000	Pakistan	Lahore	31.545	74.341
12299	Palau	Koror	7.350	134.517

Population	Country	City	Latitude	Longitude
450668	Panama	Panama City	8.967	–79.533
250000	Papua New Guinea	Port Moresby	–9.500	147.117
502426	Paraguay	Asuncion	–25.267	–57.667
7443000	Peru	Lima	–12.050	–77.050
10818000	Philippines	Manila	14.583	120.983
458053	Poland	Gdansk	54.383	18.667
3488000	Poland	Katowice	19.024	19.024
1642700	Poland	Warsaw	52.250	21.000
677790	Portugal	Lisbon	38.733	–9.133
422000	Puerto Rico	San Juan	18.467	–66.117
300000	Qatar	Doha	25.250	51.600
2351000	Romania	Bucharest	44.433	26.100
9299000	Russia	Moscow	55.750	37.700
5132000	Russia	Saint Petersburg	59.933	30.333
594701	Russia	Vladivostok	43.150	131.883
232733	Rwanda	Kigali	–1.933	30.067
32859	Samoa	Apia	–13.831	–171.752
2397	San Marino	San Marino	43.933	12.433
3328000	Saudi Arabia	Riyadh	24.650	46.767
1199629	Scotland	Glasgow	55.883	–4.250
1729823	Senegal	Dakar	14.667	–17.433
1574050	Serbia	Belgrade	44.833	20.500
25000	Seychelles	Victoria	–4.633	55.467
1300000	Sierra Leone	Freetown	8.500	–13.250
3587000	Singapore	Singapore	1.300	103.833
446600	Slovakia	Bratislava	48.167	17.167
330000	Slovenia	Ljubljana	46.067	14.500
35288	Solomon Islands	Honiara	–9.467	159.950
900000	Somalia	Mogadishu	2.033	45.350
3092000	South Africa	Cape Town	–35.917	18.367
1480530	South Africa	Johannesburg	–26.133	27.900
749921	South Africa	Port Elizabeth	–33.967	25.600
1104479	South Africa	Pretoria	–25.750	28.200
4239000	South Korea	Puan	–13.828	–171.744
11968000	South Korea	Seoul	37.533	127.000
1510000	Spain	Barcelona	41.383	2.183
4072000	Spain	Madrid	40.400	–3.683
1994000	Sri Lanka	Colombo	6.917	79.867
924505	Sudan	Khartoum	15.600	32.533
200970	Suriname	Paramaribo	5.833	–55.167
47020	Swaziland	Mbabane	–26.333	31.133
703627	Sweden	Stockholm	59.333	18.050
129423	Switzerland	Bern	46.950	7.433
1080000	Switzerland	Zurich	47.367	8.550
1549932	Syria	Damascus	33.500	36.300
2643439	Taiwan (ROC)	Taipei	25.083	121.533
524000	Tajikistan	Dushanbe	38.633	68.850

Population	Country	City	Latitude	Longitude
1360850	Tanzania	Dar es Salaam	–6.850	39.300
7221000	Thailand	Bangkok	13.733	100.500
366476	Togo	Lome	6.133	1.217
34000	Tonga	Nukualofa	–21.150	–175.233
52451	Trinidad and Tobago	Port-of-Spain	10.633	–61.517
887800	Tunisia	Tunis	36.800	10.183
3190000	Turkey	Ankara	39.917	32.833
9413000	Turkey	Istanbul	41.017	28.967
518000	Turkmenistan	Ashgabat	41.332	19.817
3839	Tuvalu	Funafut	–8.517	179.217
773463	Uganda	Kampala	0.317	35.417
7640000	UK	London	51.500	–0.167
2637000	Ukraine	Kiev	50.417	133.717
363432	United Arab Emirates	Abu Dhabi	24.467	54.367
2200000	United States	Houston	29.750	–95.367
6945000	United States	Chicago	41.883	–87.650
3912000	United States	Dallas	32.781	–96.797
1300000	United States	Denver	39.755	–104.988
3785000	United States	Detroit	42.330	–83.046
3918000	United States	Houston	–95.363	–95.363
13129000	United States	Los Angeles	34.050	–118.250
16626000	United States	New York	40.717	–74.000
4398000	United States	Philadelphia	39.952	–75.164
4051000	United States	San Francisco	37.775	–122.419
3927000	United States	Washington D.C.	–77.024	–77.024
876156	United States	Honolulu	21.300	–157.817
1330440	Uruguay	Montevideo	–34.883	–56.183
2106000	Uzbekistan	Tashkent	41.267	69.217
26100	Vanuatu	Port Vila	–17.750	168.300
3153000	Venezuela	Caracas	10.500	–66.933
345489	Venezuela	Merid	8.400	–71.133
3678000	Vietnam	Hanoi	21.017	105.867
6424519	Vietnam	Ho Chi Minh City	10.767	106.717
1972011	Yemen	Sanaa	15.400	44.233
1168454	Yugoslavia	Belgrade	41.332	19.817
1184169	Zimbabwe	Harare	–17.833	31.500

INTENTIONALLY LEFT BLANK.

Acronyms and Abbreviations

AAIM	An Army Illumination Model
As	altostratus
Ac	altocumulus
ARL	U.S. Army Research Laboratory
Cb	cumulonimbus
Ci	cirrus
Cs	cirrostratus
Cu	cumulus
DMS	degrees, minutes, seconds
HAFB	Hanscom Air Force Base
LOS	line-of-sight
LUME	Light Urban Model Effects
NVGs	night vision goggles
SBIR	Small Business Innovative Research
Sc	stratocumulus
St	stratus
UTC	coordinated universal time

NO. OF COPIES	ORGANIZATION
1 PDF	ADMNSTR DEFNS TECHL INFO CTR ATTN DTIC OCP 8725 JOHN J KINGMAN RD STE 0944 FT BELVOIR VA 22060-6218
3	ARMY RESEARCH LABORATORY ATTN IMNE ALC IMS MAIL & RECORDS MGMT ATTN AMSRD ARL CI OK TL TECHL LIB ATTN AMSRD ARL CI OK PE TECHL PUB 2800 POWDER MILL ROAD ADELPHI MD 20783-1197
1	ARMY RESEARCH LABORATORY ATTN AMSRD CI OK TP TECHL LIB APG MD 21005
1	ARMY RESEARCH LABORATORY ATTN AMSRD ARL CI DR GOWENS 2800 POWDER MILL ROAD ADELPHI MD 20783-1197
1	ARMY RESEARCH LABORATORY ATTN AMSRD ARL CI E P CLARK 2800 POWDER MILL ROAD ADELPHI MD 20783-1197
1	ARMY RESEARCH LABORATORY ATTN AMSRD ARL CI DR NAMBURU 2800 POWDER MILL ROAD ADELPHI MD 20783-1197
1	ARMY RESEARCH LABORATORY ATTN AMSRD ARL CI ED DR HOOCK BUILDING 1622 WSMR NM 88002-5501
1	ARMY RESEARCH LABORATORY ATTN AMSRD ARL CI EM D KNAPP BUILDING 1622 WSMR NM 88002-5501
2	ARMY RESEARCH LABORATORY ATTN AMSRD ARL CI EM DR SHIRKEY BUILDING 1622 WSMR NM 88002-5501
1	NAVAL RESEARCH LABORATORY MARINE METEOROLOGY DIVISION DR A GOROCH 7 GRACE HOPPER AVE MONTEREY CA 93943
3	US ARMY NATICK SOLDIER CENTER MR ROBERT AUER KANSAS STREET NATICK MA 01760
1	NORTHROP GRUMMAN MS M GOUVEIA 100 BRICKSTONE SQUARE ANDOVER MA 01810
1	ATMOSPHERIC ENVIRONMENTAL RESEARCH INC DR G SEELEY 131 HARTWELL AVENUE LEXINGTON MA 02421-3136
1	SCIENCE APPLICATIONS INTERNATIONAL CORPORATION LEANDRO DELGADO 731 LAKEPOINTE CENTRE DRIVE O'FALLON IL 62269-3064
3	US ARMY NATICK SOLDIER RD&E CENTER ATTN AMSRD NSR TS M B AUER 15 KANSAS STREET NATICK MA 01760-5056
1	DIRECTOR, USA TRAC ANALYSIS CENTER ATTN ATRC FMA T GACH 255 SEDGWICK AVE FORT LEAVENWORTH KS 66027-2345

NO. OF COPIES	ORGANIZATION
1	DIRECTOR, USA TRAC ANALYSIS CENTER ATTN ATRC FMA S GLASGOW 255 SEDGWICK AVE FORT LEAVENWORTH KS 66027-2345
1	DIRECTOR, USA TRADOC ANALYSIS CENTER ATTN ATRC WEC D DURDA WSMR NM 88002-5502

TOTAL: 25 (1 PDF, 24 CDS)

INTENTIONALLY LEFT BLANK.